Developments in Environmental Science, volume 2, pp. 165–194
ISSN: 1474-8177
Published by Elsevier Science Ltd.

Chapter 7

Use of auxiliary data for spatial interpolation of surface ozone patterns

E. Henry Lee

US Environmental Protection Agency, Western Ecology Division, 200 SW 35th Street, Corvallis, OR 97333, USA
E-mail: lee.ehenry@epa.gov

Abstract

The spatial pattern of tropospheric ozone in the Sierra Nevada and surrounding Central Valley was interpolated to the surface of a digital elevation model at 1-km resolution by using sampled data from continuous ozone monitors and passive samplers in conjunction with auxiliary data for temperature. The network of passive samplers supplemented the active monitoring network to provide a more accurate ozone prediction surface in the Sierra Nevada for identifying the geographic locations at potential ecological risk. The passive sampler data indicated much higher ozone concentrations in the higher elevations of the Sierra Nevada than predicted based on only the continuous monitoring data. Prevailing westerly to northwesterly winds transported pollutant plumes from major urban sources in the southern latitudes of the San Joaquin Valley toward the Sierra Nevada foothills, where seasonal mean ozone concentrations were higher than in the low-elevation Central Valley region sheltered by the Coastal range. The leave-one-out cross-validation bias was −0.1 ppb, and the mean absolute error was 6.3 ppb for the mean ozone concentration for the June 9 to September 15, 1999 period.

1. Introduction

The spatial distribution of tropospheric ozone (O_3) is difficult to infer in mountainous regions due to sparse coverage of the air quality monitoring network and the complexity of O_3 transport phenomena and chemistry (Lee and Hogsett, 2001). Spatial interpolation of O_3 patterns is based primarily on a network of continuous monitors conducted by state and local agencies for regulatory purposes. Most continuous O_3 monitoring sites in the United States are located within or in the immediate proximity of urban and low-elevation areas

(Chameides et al., 1997; Saylor et al., 1998; Demerjian, 2000). Few continuous monitors are located in rural and high-elevation areas distant from urban pollutant sources due to budget, personnel constraints and the unavailability of a source of power. Ambient O_3 concentrations near urban areas display a strong diurnal pattern with morning and evening concentrations near zero and maximum concentrations in the afternoon. In contrast, O_3 concentrations in high-elevation and rural locations typically have a flatter diurnal pattern with higher nighttime concentrations than that for urban areas (Wolff et al., 1987; Böhm et al., 1991, 1995; Guttorp et al., 1994; Peterson et al., 1999). Concerns about the spatial representativeness and operating cost of the network of continuous monitoring sites have prompted the use of low-cost passive samplers to investigate the spatial distribution of O_3 in national parks and rural areas (Ray, 1993, 1996, 2001; Ray and Flores, 1994; Brace and Peterson, 1998; Peterson et al., 1999; Cooper and Peterson, 2000). The advent of passive samplers in field settings provides auxiliary data for quantifying spatial patterns of tropospheric O_3 in complex terrain.

Local topographical features and their effect on transport of polluted air have a significant influence on the diurnal pattern of O_3 concentrations. At six remote monitoring stations on the western slope of the Sierra Nevada in California, three stations displayed a weak diurnal pattern typical of a high-elevation, remote site; and three stations exhibited a distinct diurnal pattern characteristic of a low-elevation urban area (Van Ooy and Carroll, 1995). Differences in diurnal patterns were attributed to topographic setting and its effect on wind patterns rather than distance downwind from a major urban source. In complex terrain, diurnal signatures and their mean O_3 concentrations may vary within short distances between areas of different altitudes or topography. Spatial variations in O_3 concentrations occur in the 10- to 50-km range in complex terrain (Ray, 2001). The poor spatial resolution and distribution of the network of continuous monitors limits the ability to resolve the spatial variability of mean O_3 concentrations in the Sierra Nevada range where daily maximum O_3 concentrations frequently exceed 100 ppb during the summer months. Recently, a network of O_3 passive samplers have been established to provide a much improved spatial representation of air quality in the Sierra Nevada region of California.

Ogawa passive samplers containing nitrite-coated filters have been tested under laboratory and field conditions and shown to provide an accurate and inexpensive measurement of mean O_3 concentration (or total concentration) in field settings (Zhou and Smith, 1997). The National Park Service reported that passive samplers were accurate to within $\pm 10\%$ of the weekly average O_3 concentrations obtained by using continuous monitors over a variety of terrain and weather conditions (Ray, 2001). The USDA Forest Service's Pacific Southwest Research Station (FS PSWRS) established a network of O_3 passive

samplers at higher-elevation, remote sites (440 m to 2790 m) with a limited number of collocated electronic analyzers in the Sierra Nevada region in 1999. The passive samplers provided data on a 2-week basis from mid-May to mid-October 1999.

In this study, we examined the use of passive samplers to better predict the spatial pattern of tropospheric O_3 concentrations in the Sierra Nevada study area. The elevation-based spatial interpolation approach utilized auxiliary data from more intensely sampled correlated variables (i.e., elevation, temperature) to predict air quality over broad spatial scales (Lee and Hogsett, 2001). This was accomplished primarily through the use of loess regression to model O_3 concentrations as a nonparametric function of elevation, temperature, and geographic coordinates. We illustrated the spatial interpolation approach to predict the mean O_3 concentration for the June 9 to September 15, 1999 period by using the continuous monitor data alone and in conjunction with the passive sampler data. When the continuous monitor data were used to calibrate the loess model, the passive sampler data were used to examine the accuracy and precision of the spatial predictions. The mean O_3 prediction surfaces and their standard deviations (SDs), excluding and including the passive sampler data in the loess fit, were compared to measure improvements in interpolation accuracy and precision.

2. Methods

The study area includes the Sierra Nevada of California and the surrounding Central Valley where the majority of continuous O_3 monitoring sites were located (Fig. 1). The Sierra Nevada range rises steeply from the Great Basin on its eastern front and descends gradually to the foothills bordering the Central Valley on its western slope. The study area is physically, climatically and biologically diverse, ranging from a hot, arid desert regime in the south to a Mediterranean regime with long dry summers and wet winters in the low-lying fertile basin of the Central Valley and the Sierra Nevada. Dense forests of ponderosa pine, Jeffrey pine, mixed conifer, and red and white fir cover much of the Sierra Nevada. The study area is approximately 780 km in length and 190 km in width and includes Lassen, Sequoia, Kings Canyon, and Yosemite National Parks and the Sequoia, Tahoe and Sierra National Forests. Elevation ranges from below sea level to 4418 m, including several prominent peaks greater than 4000 m in the High Sierra.

Temperatures generally decrease and mean O_3 concentrations typically increase with increasing elevation (< 1500 m) in mountainous regions (Dodson and Marks, 1997; Brace and Peterson, 1998; Bytnerowicz et al., 1999; Cooper

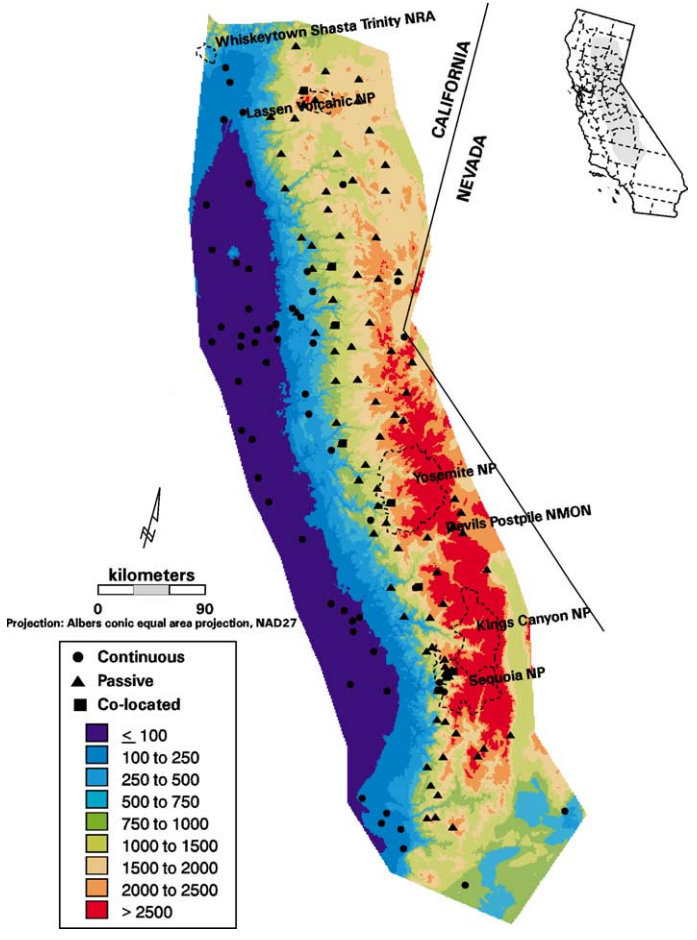

Figure 1. Location of continuous ozone monitors primarily from US Environmental Protection Agency's (EPA) Aerometric Information Retrieval System (AIRS) database and passive samplers from the USDA Forest Service's Pacific Southwest Research Station for 1999 in the Sierra Nevada study area. Elevation data (m) are from the USGS Conterminous US AVHRR digital elevation model sampled at 1-km resolution.

and Peterson, 2000). Mean O_3 concentrations in the Sierra Nevada range generally level off or decrease at higher elevations (Bytnerowicz, personal commun.). Because elevation and temperature data are widely available at higher spatial resolution than the continuous O_3 monitoring network and have been shown to correlate well with mean O_3 concentrations, these auxiliary variables were employed to improve the accuracy and precision of the mean O_3 prediction surface in complex terrain. Elevation data were from the US Geologi-

cal Survey (USGS) Conterminous Advanced Very High Resolution Radiometer (AVHRR) database resampled to 1-km resolution on an Albers equal-area conic map projection (Loveland et al., 1991).

2.1. Passive ozone sampler data

A rural network of 89 passive O_3 samplers was established by the USDA FS PSWRS in the Sierra Nevada to augment the spatial coverage of the continuous O_3 monitoring network in the Sierra Nevada (Fig. 1). Nine of the passive sampler sites were collocated with continuous O_3 monitors from two companion projects under joint arrangement between the USDA FS and California Air Resources Board, the Forest Ozone Response Study (FOREST), and the Sierra Cooperative Ozone Impact Assessment Study (SCOIAS). The data taken by passive samplers are the amounts of nitrate (NO_3^-) ion formed from nitrite (NO_2^-) ion by O_3 oxidation divided by the time of exposure, denoted as "nitrate formation rate" in ngNO_3^-/h. Field technicians changed the sampler filters within 2 days of each other so that each sampler's exposure time would be as close to 2 weeks as possible (with the exception of four National Park Service (NPS) sites in the Yosemite National Park that were exposed for 1-week periods). The field study spanned eleven 2-week periods from May 13 to October 13, 1999. Calibrations were made against the active monitors collocated with passive samplers to determine the rate of the chemical reaction to convert the oxidation rate to a mean O_3 concentration based on regression analysis. That is, the 2-week mean O_3 concentration at any given site was calculated as the product of the nitrite oxidation rate and the conversion factor.

Prior to spatial interpolation of the data, the passive sampler data were screened for outliers due to analytical error, contamination of the nitrite-coated filter, interference with other atmospheric oxidants collected by the sampler, and meteorological effects on the sampling rate and chemical reaction performance. Passive sampler sites with no collocated monitor were paired with the nearest continuous monitoring site from the US Environmental Protection Agency's (EPA) Aerometric Information Retrieval System (AIRS) network within 30 km and roughly the same elevation. Extreme nitrate formation rates (< 8 or > 29 ngNO_3^-/h) and several low formation rates (< 12 ngNO_3^-/h) were identified as outliers and excluded from the analysis due to inconsistencies with auxiliary correlated variables from neighboring passive sampler and continuous monitoring sites. High formation rates may have been caused by the collection of other atmospheric oxidants, including oxides of nitrogen and sulfur by the passive sampler (Zhou and Smith, 1997). At high wind speeds (> 10 m/s), the Ogawa samplers may overestimate O_3 concentrations by 10 to 30% (Bytnerowicz, personal commun.). Low formation rates may have been

caused by low wind turbulence at the face of the passive sampler or may have been below the detection limits of the laboratory analytical method.

For illustration of the spatial interpolation method incorporating passive sampler data, we focused on the 16-week period from June 9 to September 29, 1999, when passive samplers were in full operation at the 89 sites. The seasonal mean O_3 concentration was calculated as the mean oxidation rate over the eight 2-week periods multiplied by the conversion factor. Sites with at least six 2-week oxidation rates available in the June 9 to September 29, 1999 period were retained in the analysis.

2.2. Continuous ozone monitoring data

Hourly O_3 monitoring data from the US EPA's AIRS database and the USDA FS PSWRS's FOREST and SCOIAS networks were used in this analysis to examine and predict the mean O_3 concentration on the surface of a digital elevation model (DEM). The continuous monitoring sites were located primarily in urban areas at lower elevations (< 2208 m) west of the Sierra Nevada (Fig. 1). The EPA's AIRS database consisted of 1098 stations nationwide in 1999, of which 61 were located in the Sierra Nevada study area (Fig. 1). The AIRS database included monitoring sites in the national parks established by the NPS Air Resources Division. With the exception of four continuous monitoring stations that were collocated with the USDA FS passive samplers, all monitoring stations from other sources were already included in the AIRS database.

Two-week mean O_3 concentrations were calculated based on the average start and end date/times for the passive samplers and averaged over the June 9 to September 29, 1999, periods to derive a seasonal mean O_3 concentration. A mean O_3 concentration was set to missing when there were fewer than 75% of the hourly O_3 concentrations available in a 2-week exposure period. The seasonal mean O_3 concentration was set to missing when two or more of the 2-week means were missing. The seasonal mean index provided the best interpolation results when data for passive samplers and continuous monitors were combined to fit a loess model. The spatial interpolation analysis can be applied to the 2-week mean O_3 index but the analysis is more accurate and precise when there are no differences in the exposure periods between the passive sampler sites.

2.3. Temperature data

Daily maximum temperature data were obtained from three sources, the National Climatic Data Center (NCDC) Summary of the Day database from Earthinfo (Earthinfo, 1992), the National Interagency Fire Management Integrated Database (NIFMID) from the USDA National Information Technology

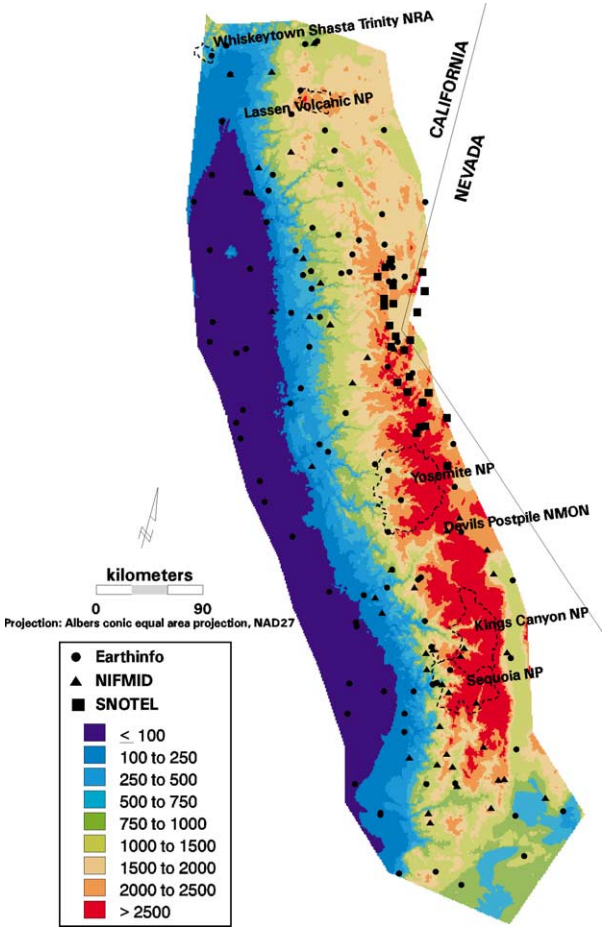

Figure 2. Location of meteorological monitors from Earthinfo's NCDC Summary of the Day, NIFMID and National Resources Conservation Service SNOTEL databases for 1999 in the Sierra Nevada study area. Elevation data (m) are from the USGS Conterminous US AVHRR digital elevation model sampled at 1-km resolution.

Center, and the National Resources Conservation Service (NRCS) SNOTEL network (Fig. 2). The Earthinfo database consists of five daily climatological parameters in the NCDC's TD-3200 database for over 19,000 weather stations in the US, primarily from the National Weather Service. The NIFMID weather data come from a network of remote automatic weather stations (RAWS) and automatic weather stations (AWS) operated by seven federal agencies involved with forest fire management. The RAWS units collect, store, and transfer data (via satellite) hourly to a central computer system while

AWS units use telephone telemetry to transfer data on a daily basis. Daily maximum temperature data for 26 NRCS SNOTEL meteorological stations were obtained from the Western Regional Climate Center (WRCC) Web site http://www.wrcc.dri.edu/index.html. The 99 NCDC meteorological stations in the study area were distributed at lower elevations than the NIFMID and SNOTEL stations that were located within the Sierra Nevada. Only 6% of the NCDC stations were at elevation greater than 2000 m versus 19% of the NIFMID stations and 85% of the SNOTEL stations.

Many studies have found that ambient air temperature was the most important meteorological variable for modeling trends in mean or peak O_3 concentrations or identifying peak O_3 days (Wolff and Lioy, 1978; Chock et al., 1982; Kuntasal and Chang, 1987; National Research Council, 1992; Eder et al., 1994; Van Ooy and Carroll, 1995). The monthly mean daily maximum temperature was a key predictor variable for the interpolation of monthly SUM06 in non-urban areas in the US (Lee and Hogsett, 2001). The daily maximum temperatures were averaged initially across a 2-week period in accordance with the passive sampler schedule. The seasonal mean temperature for June 9 to September 29, 1999, was calculated as the average of the 2-week mean temperatures. The mean daily maximum temperature variable was chosen because: (1) the correlation between mean O_3 concentrations and temperature was generally the strongest and was stable over time and space, (2) an elevation-based method exists for interpolating temperature over complex terrain, and (3) temperature data were widely available at sufficient resolution and coverage in space and time.

2.4. Spatial interpolation of temperature and ozone

An elevation-based spatial interpolation method was used to predict temperature and O_3 concentrations over complex terrain and account for the orographic effects on the regionalized variables of interest (Lee and Hogsett, 2001). Loess regression was used to model the spatial variability of the variable of interest as a function of elevation, geographic location, and other auxiliary, highly-correlated variables. The loess model used for estimating the mean O_3 concentration (Y_i in ppb) at site i is

$$Y_i = g(easting_i, northing_i, temp_i, elev_i) + \varepsilon_i \quad (1)$$

where $easting_i$ and $northing_i$ are the Albers projection coordinates, $temp_i$ is the mean daily maximum temperature (in °C), $elev_i$ is elevation (in m) and ε_i is the model error with mean zero and variance Φ. The regression surface $g(\cdot)$ was assumed to be locally well approximated by a quadratic polynomial that includes first- and second-order terms for the predictors and their interactions in a neighborhood specified by the loess parameter $\alpha(> 0)$; larger values of α

result in a larger neighborhood size and a smoother loess prediction surface (Cleveland, 1979; Cleveland et al., 1992). The second-order monomials for temperature and elevation (*temp*, *elev*) were omitted from the model based on parsimony and adequacy of fit. The regression surface was assumed to be conditionally parametric in temperature. In other words, the regression surface for O_3 has the form

$$\begin{aligned} & g(easting_i, northing_i, temp_i, elev_i) \\ & \quad = \beta_0(easting_i, northing_i, elev_i) \\ & \qquad + \beta_1(easting_i, northing_i, elev_i) * temp_i \end{aligned} \tag{2}$$

where $\beta_0(\cdot)$ and $\beta_1(\cdot)$ are nonparametric smooth functions to be determined by the data.

Because O_3 and temperature data have different support points, the mean daily maximum temperature values at the continuous monitoring and passive sampler sites must be spatially interpolated. The loess model for temperature is

$$temp_i = h(easting_i, northing_i, elev_i) + v_i \tag{3}$$

where v_i is the model error with mean zero and variance σ^2 and $h(\cdot)$ is approximated by a locally quadratic polynomial in the Albers projection coordinates and elevation. The loess model for temperature was assumed to be conditionally parametric in elevation, i.e.,

$$\begin{aligned} & h(easting_i, northing_i, elev_i) \\ & \quad = \gamma_0(easting_i, northing_i) + \gamma_1(easting_i, northing_i) * elev_i \\ & \qquad + \gamma_2(easting_i, northing_i) * elev_i^2 \end{aligned} \tag{4}$$

where $\gamma_0(\cdot)$, $\gamma_1(\cdot)$ and $\gamma_2(\cdot)$ are nonparametric smooth functions to be determined by the data. The loess predictions for temperature in conjunction with elevation and the Albers projection coordinates were used to predict mean O_3 concentrations based on the continuous monitoring data, alone and in conjunction with the passive sampler data. The efficacy of the passive sampler data for predicting mean O_3 concentrations is examined by comparing the surfaces for mean O_3 predictions and the SD for loess surface estimation with and without the passive sampler data. Kriging was used to check for small-scale spatial dependencies among the loess residuals for mean temperature and mean O_3 concentrations. A "spherical" variogram model was used to model the covariance structure as a function of relative spatial location. Weighted nonlinear least squares was used to fit a theoretical variogram model to the empirical one (Cressie, 1985). When small-scale spatial dependencies were observed, the

loess and kriged predictions were summed to produce an optimal prediction at a nonsampled point as a weighted function of surrounding sampled points. The two methods used different approaches for the assignment of weights to the neighboring support points. In both methods, the weights decreased as the relative spatial distance from the point of interest increased. All calculations were performed in MathSoft Splus V6.0.1 and its accompanying module S+Spatialstats V1 (MathSoft, 1996, 2000).

The loess and kriged predictions are both linear in the variable of interest. This linearity property results in distribution properties of the predictor that are analogous to classical parametric procedures and facilitates calculation of the prediction variance or SD. Under the assumption of Gaussian error with mean 0 and variance ϕ^2, the prediction SD or prediction interval at nonsampled points may be used to quantify the precision of the interpolation procedure. When kriging was not required, the prediction SD is $\{\phi^2 + \textit{variance for loess surface estimation}\}^{1/2}$, where ϕ^2 is the loess residual variance. When kriging was required, the prediction SD is $\{\textit{variance for loess surface estimation} + \textit{variance for kriged prediction}\}^{1/2}$. The network sampling design affects the precision of the spatial prediction via the variance (or SD) for loess surface estimation.

3. Results and discussion

3.1. Relationship between nitrate formation rate and ozone concentrations

Simple linear regression with zero intercept was used to relate 2-week mean O_3 concentration and nitrate formation rate based on eight Ogawa passive samplers collocated with each of the FOREST/SCOIAS continuous monitors and eleven 2-week sampling periods from May 13 to October 13, 1999 (Fig. 3). Formation rates at Shaver Lake were excluded from the regression analysis because Shaver Lake had a much different O_3–nitrate formation rate relationship than the other collocated passive sampler sites. Data from all time periods were combined to fit a common regression model. The conversion factor (i.e., slope) was 3.311 (standard error [S.E.] = 0.035) for the collocated passive sampler sites. Another 34 passive samplers had an AIRS monitor within 30 km with Pearson correlation between formation rate and O_3 concentrations greater than 0.5. The conversion factor (slope = 3.222, S.E. = 0.038) for these 34 passive sampler sites with neighboring AIRS monitors was not significantly different at the 0.05 level of significance to that for the eight passive sampler sites with collocated monitors based on weighted least squares analysis (P-value = 0.086). Although the O_3-nitrate formation rate relationship could be inferred from passive sampler and neighboring continuous monitoring data, the variation about the regression line was 5.5 times greater than that for the

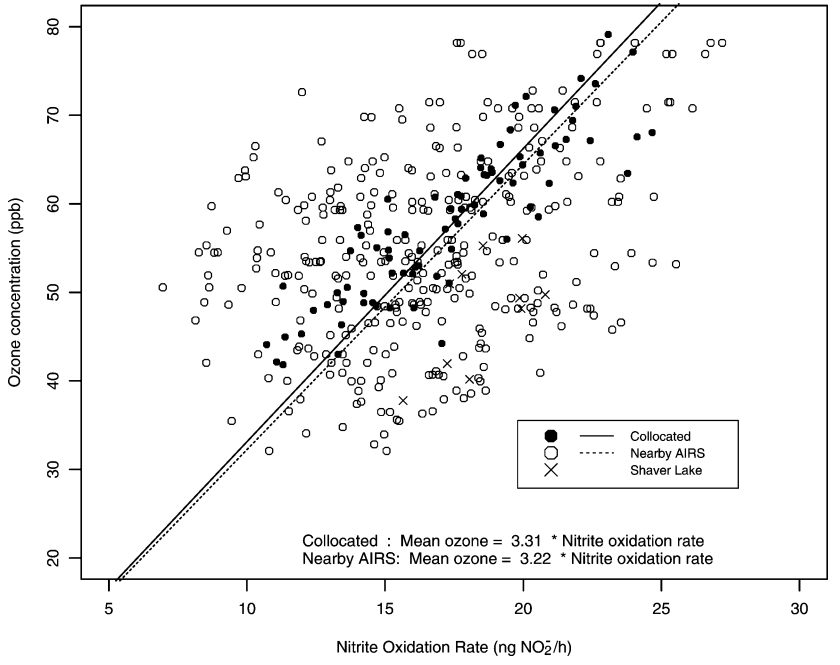

Figure 3. Linear relationship between nitrate formation rates and mean ozone concentrations for eleven 2-week periods between May 13 and October 13, 1999. Mean ozone concentrations correspond to either collocated FOREST continuous monitors at eight passive sampler sites or the nearest US EPA AIRS monitoring site within 30 km of the passive sampler site. The passive sampler site at Shaver Lake was excluded from the regression analysis.

passive samplers collocated with FOREST and SCOIAS monitors. The decreased precision in fit was largely due to the non-uniform distribution of O_3 in complex terrain. Ozone spatial distribution studies in California and national parks in the western US reported substantial variations in O_3 concentrations in the 10- to 50-km range (Ray, 2001).

The nitrate formation rates were converted to 2-week mean O_3 concentrations based on the regression fit for collocated sites. The passive samplers were accurate to within $\pm 28\%$ of the 2-week mean O_3 concentrations for the collocated continuous monitors; about 85% of the mean O_3 concentration values for the passive samplers were within $\pm 10\%$ of the mean O_3 values for the collocated continuous monitors. For the 2-week exposures, the mean absolute percent difference between the passive samplers and collocated continuous monitors data was 7.6% ($n = 81$). In comparison, the NPS reported a mean absolute percent difference less than 10% for weekly passive sampler data at collocated sites in seven western parks (Ray, 2001). Accuracy for the passive sampler data in the Sierra Nevada improved when seasonal mean O_3 concentrations for

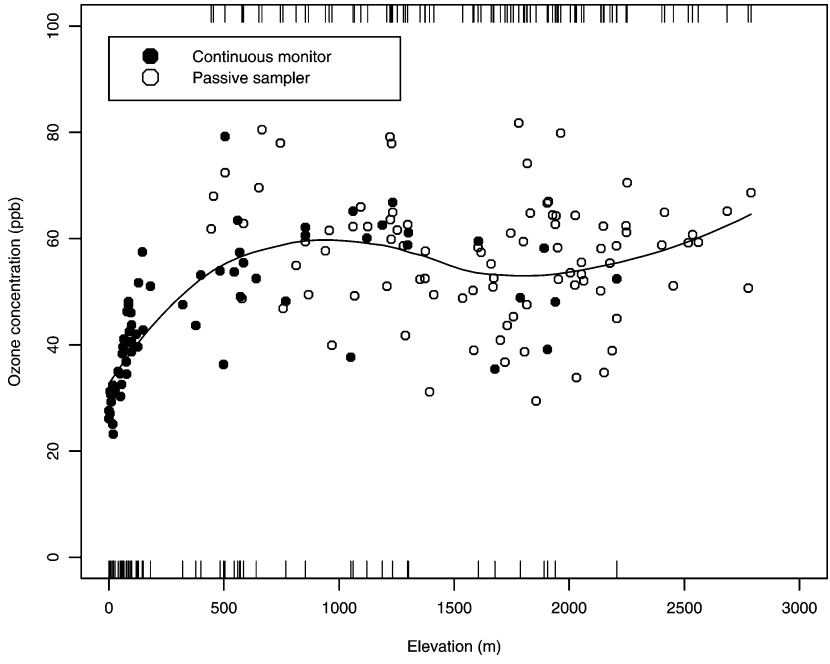

Figure 4. Mean ozone concentrations for June 9 to September 29, 1999 period versus elevation for continuous ozone monitors and passive samplers in the Sierra Nevada study area. The distribution of elevations for the active monitors is displayed on the bottom while that for the passive sampler sites is displayed on the top.

June 9 to September 29, 1999, were considered. The percent difference in the seasonal mean O_3 concentrations between the eight passive samplers and continuous monitors ranged from −6.6% to 14.2%, and the mean absolute percent difference was 5.8%.

Seasonal mean O_3 concentrations in the Sierra Nevada study area typically increased with elevation before leveling off at higher elevations, although there was considerable variability in the passive sampler data (Fig. 4). A similar pattern was observed in the San Bernardino Mountains where mean O_3 concentrations typically increased with elevation up to about 1500 m and then gradually decreased with elevation (Bytnerowicz et al., 1999). Low seasonal mean O_3 concentrations were generally associated with a strong diurnal pattern due to scavenging of O_3 by NO near the photochemical smog sources areas. Nighttime hourly O_3 concentrations were generally higher for the remote higher-elevation passive sampler sites than for the lower-elevation continuous monitoring sites in close proximity to major urban areas. Consequently, the seasonal mean O_3 concentrations were higher for the passive sampler sites due to the greater contribution of nighttime hourly O_3 concentrations to the overall mean.

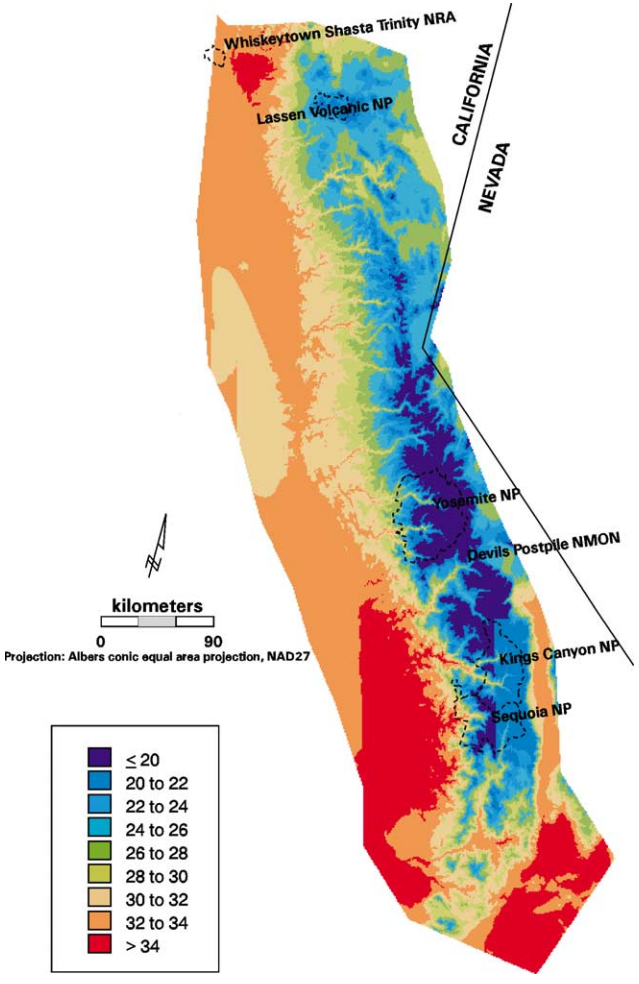

Figure 5. Predicted mean daily maximum temperature (°C) for the Sierra Nevada study area for the June 9 to September 29, 1999 period.

3.2. Spatial prediction for temperature

A locally quadratic loess fit was used to relate seasonal mean daily maximum temperature from the NCDC, NIFMID, and SNOTEL databases as a function of elevation and geographic location. The loess fit with smoothing parameter $\alpha = 0.5$ explained much of the variation in temperature ($r^2 = 0.94$) and had a residual standard error (RSE) equal to 1.4 °C. Because small-scale spatial

dependencies were not found in the loess residuals, kriging was not required to predict temperature. In previous studies, kriging of the loess residuals resulted in negligible improvement in accuracy and precision of the spatial prediction for monthly mean daily maximum temperature in the western US (Lee and Hogsett, 2001). Temperature at unsampled points on a 1-km grid of the DEM surface was interpolated based on neighboring sampled points weighted according to the loess fit.

The spatial pattern for predicted seasonal mean temperature had the expected elevational gradients and was consistent with local topographical features (Fig. 5). Temperatures displayed an east–west gradient consistent with warmer temperatures in the fertile basin of the Central Valley, decreasing with increasing elevation to a minimum at higher elevations greater than 2500 m in the northeastern section of the Sierra Nevada mountain range. Lower temperatures were predicted in the northwestern region of the Central Valley in the rain shadow of the Northern Coastal Range to the west. The highest temperatures ($> 34\,^{\circ}$C) were predicted in the low-elevation Mojave Desert region in the southernmost portion of the study area. Seasonal mean daily maximum temperatures at elevation greater than 2000 m in the Sierra Nevada range varied from 15 °C to 29 °C with a mean of 21.7 °C.

3.3. Cross-validation of loess predictions for temperature

When the sampled point was excluded and the loess regression refit to the remaining points, the loess predictions for temperature were nearly unbiased and precise to within 1.5 °C on average (Table 1). The leave-one-out cross-validation errors ranged from $-5.0\,^{\circ}$C to 4.8 °C with a mean error (i.e., bias) equal to 0.0 °C and a mean absolute error (MAE) equal to 1.2 °C. About 95% of the predicted temperatures were within the limits of the 95% prediction interval. The loess predictions based on neighboring sampled points were highly correlated with the observed temperatures ($r = 0.96$). Our spatial predictions for 1999 mean temperature for the Sierra Nevada and surrounding area were comparable in accuracy and precision to that for the June 1990 mean temperature for central California (Lee and Hogsett, 2001). The NIFMID sites distributed at lower elevations in the Sierra Nevada with temperatures greater than 23 °C were underpredicted by 1.1 °C on average. On the other hand, the loess predictions for the high-elevation SNOTEL sites in the northern section of the Sierra Nevada with local maximum temperatures less than 26 °C were nearly unbiased. Meaningful relationships were not found between the cross-validation residuals and the predictor variables, indicating that the loess fit for temperature was adequate for spatial interpolation across the study area.

Table 1. Summary of the leave-one-out cross-validation results for the loess prediction of mean daily maximum temperature (June 9 to September 29, 1999) based on the Earthinfo, NIFMID, and SNOTEL meteorological stations

Data	Sample size	Minimum observed, predicted (°C)	Maximum observed, predicted (°C)	Mean observed, predicted (°C)	Mean error (°C)	Mean |error| (°C)	Jackknife std. error (°C)	Mean pred. SD (°C)	% of errors within 95% pred. interval	Correlation obs. vs. predicted
Earthinfo	99	21.4, 23.1	37.4, 36.7	30.7, 31.2	−0.44	1.03	1.31	1.54	0.95	0.94
NIFMID	47	22.9, 21.4	39.0, 35.7	30.6, 29.5	1.09	1.52	1.56	1.53	0.91	0.93
SNOTEL	26	17.1, 17.8	25.8, 25.1	21.1, 21.3	−0.18	0.94	1.11	1.51	1.00	0.88
Overall	172	17.1, 17.8	39.0, 36.7	29.2, 29.2	0.03	1.15	1.51	1.54	0.95	0.96

Table 2. Locally quadratic loess fits for mean ozone concentrations for the June 9 to September 29, 1999 period as a function of elevation, geographic location, and mean temperature based on the network of continuous ozone monitors, alone and in conjunction with the network of passive samplers in the Sierra Nevada study area

Data	Sample size	Residual std. error (ppb)	r^2	Span α	Coefficient of variation (%)
Continuous monitor	62	4.6	0.88	1.2	10.4
Continuous monitor & passive sampler	143	7.4	0.71	1.1	14.3

3.4. Spatial prediction for ozone

A locally quadratic loess regression model was used to spatially interpolate the mean O_3 concentration for the 8-week period between June 9 and September 29, 1999. The seasonal mean daily maximum temperature was predicted at the continuous monitor and passive sampler sites by using the loess fit and was included as a predictor variable in the loess regression for ozone. Initially, the loess nonparametric regression procedure was applied to the continuous monitoring data primarily from the US EPA's AIRS database. The optimum loess fit had $r^2 = 0.88$ (Table 2). Because examination of the loess residuals indicated no signs of spatial dependencies, kriging was not required for spatially interpolating mean O_3 concentrations. In a previous study, kriging of the loess residuals resulted in marginal improvements in the accuracy and precision of the spatial predictions for the monthly SUM06 O_3 exposure index for the western US (Lee and Hogsett, 2001).

The locally quadratic loess fit using the continuous monitoring sites was able to resolve O_3 features in the western half of the study area, but the prediction surface for O_3 was less detailed in the eastern half where spatial coverage was lacking (Fig. 6). Blank areas on the prediction surface for O_3 indicated points on the DEM surface that were outside the range of the sampled data; thus, loess predictions were not possible. The highest mean O_3 concentrations were predicted in the southern latitudes in the San Joaquin Valley (SJV), downwind from nearby major urban areas. High O_3 concentrations were also predicted in the mid-latitudes in the fertile basin of the great Central Valley west of the Sierra Nevada. The lowest mean O_3 concentrations were predicted in the northern latitudes of the Sierra Nevada where temperatures were lowest and pollutant plumes transported from urban sources were minimal. Low O_3 concentrations were also predicted in the Central Valley region in the rain shadow of the northern and southern Coastal Ranges to the west that formed a natural barrier between the coast and the interior.

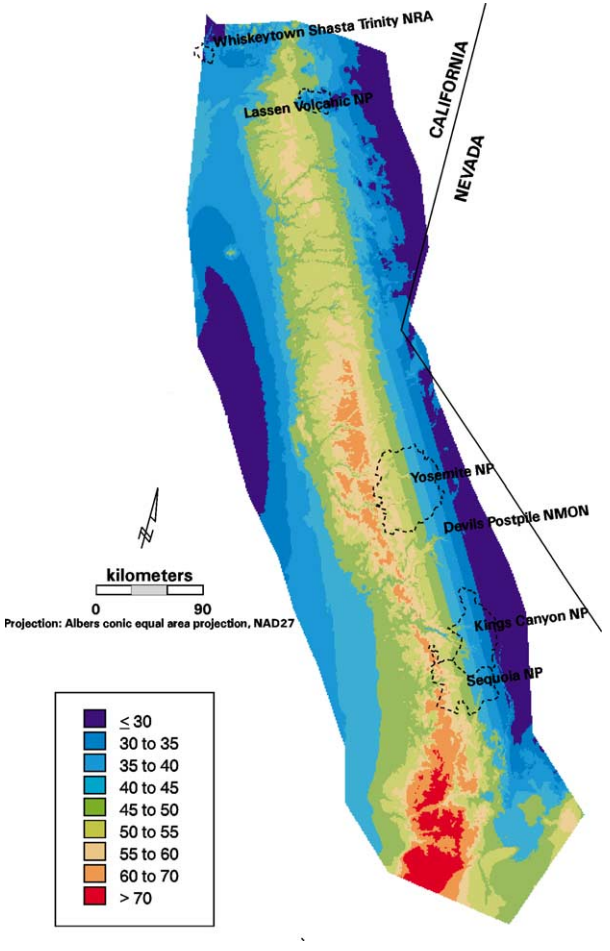

Figure 6. Predicted mean ozone concentration (ppb) for Sierra Nevada study area for the June 9 to September 29, 1999 period based on the network of continuous monitors primarily from the US EPA AIRS database.

The loess prediction SDs displayed an east–west gradient, increasing with elevation and distance from the sampled points (Fig. 7). The highest prediction SDs was located at higher elevations in the Sierra Nevada and along the eastern periphery of the study area where spatial coverage in the continuous monitoring network was lacking. The passive sampler sites filled in many gaps in the continuous monitoring network and were located at higher elevations in the Sierra Nevada where the accuracy and precision of the predicted O_3 surface

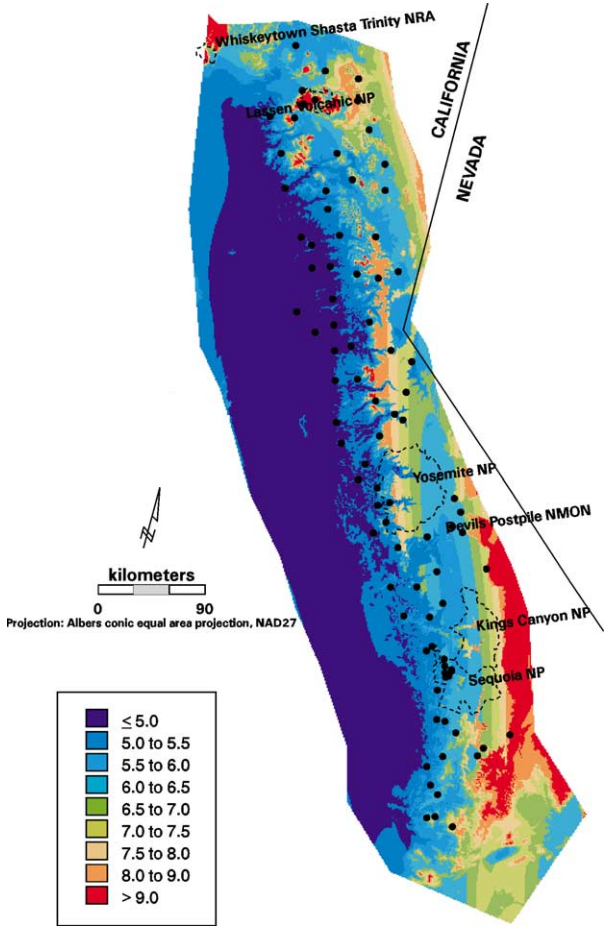

Figure 7. Standard deviation for predicted mean ozone concentration (ppb) for the Sierra Nevada study area for the June 9 to September 29, 1999 period based on network of continuous monitors primarily from the US EPA AIRS database. Points on the map indicate the location of the auxiliary passive sampler sites from USDA Forest Service's Pacific Southwest Research Station.

were poor. However, there were areas along the eastern periphery that were largely unsampled.

When the passive samplers were combined with the continuous monitors, the loess fit had $r^2 = 0.71$ and RSE $= 7.4$ ppb (Table 2). The loess fit for the combined data was worse than that for the continuous monitor data because the higher sampling density of the combined data resulted in greater resolution of the spatial variations in mean O_3 concentrations in the Sierra Nevada.

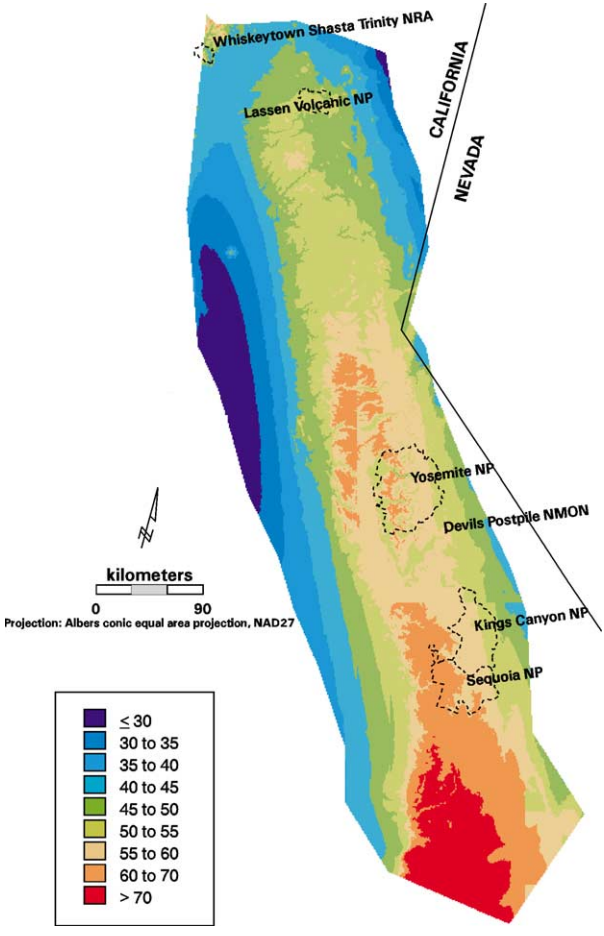

Figure 8. Predicted mean ozone concentration (ppb) for Sierra Nevada study area for the June 9 to September 29, 1999 period based on combined data for continuous monitors and passive samplers.

Mean O_3 concentrations were less uniform in the Sierra Nevada than in the low-lying fertile basin of the Central Valley. The spatial pattern for predicted mean O_3 concentrations on a 1-km grid of a DEM surface had greater detail and accuracy in the eastern half of the study area when passive samplers were included in the loess fit (Fig. 8). In particular, higher mean O_3 concentrations were predicted in the Sierra Nevada where nighttime concentrations were typically higher due to minimal O_3 titration in rural areas (Logan, 1989; Böhm et al., 1991, 1995). While air quality in the Lake Tahoe Basin in the northern

end of the Sierra Nevada is the product of local pollution sources, air quality in most other areas in the Sierra Nevada is due to long-range pollutant transport (Miller, 1996). Ozone concentrations in the Sierra Nevada range increased with elevation up to about 1500 m and then gradually decreased with elevation. The orographic effects on O_3 in the Sierra Nevada were similar to those observed in the San Bernardino Mountains (Bytnerowicz et al., 1999). Mountains extending above the boundary layer (1000 to 2000 m during the day to as low as 100 m at night) act as barriers to pollutant transport (Oke, 1990). The highest O_3 concentrations occurred in the southern latitudes in the SJV where meteorological conditions are conducive to O_3 formation and the surrounding mountains to the east serve as a barrier to pollutant transport. The extended plume of high mean O_3 concentrations in the SJV indicated that O_3 was transported at high concentrations over long distances within the subsidence inversion layer (Edinger, 1973; Ludwig et al., 1995; Fujioka et al., 1999). Layers containing O_3 may extend to 3000 m in height in the Los Angeles basin, well above the nighttime inversion layer of 600 m (Miller et al., 1986). The O_3 within the subsidence layer was intercepted by the high terrain in the foothills of the Sierra Nevada over distances of several hundred kilometers or more from the urban source. Lower O_3 concentrations occurred in the Central Valley in the rain shadow of the Coastal Ranges where there were no major urban pollutant sources and temperatures were lower than in the interior.

The O_3 predictions were much less precise across the study area because of increased spatial variability in mean O_3 concentrations in the combined data set. The prediction SD surface was uniformly high (> 7.5 ppb) across the study area and was dominated by the large loess residual variance component ($= 7.4$ ppb) (Fig. 9). The highest prediction SDs were located in the southeastern part of the study area on the leeward side of the steep eastern front of the Sierra Nevada, where spatial coverage was most lacking and elevation gradients were severe. In the Sierra Nevada, elevation changed rapidly over short distances resulting in abrupt shifts in diurnal patterns and mean O_3 concentrations.

The inclusion of the passive sampler data resulted in higher mean O_3 predictions in the Sierra Nevada and little to no change in the O_3 prediction surface in the Central Valley (Fig. 10). In particular, the accuracy of the mean O_3 predictions at unsampled points along the leeward side of the eastern front of the Sierra Nevada range improved significantly when the passive sampler data were added to the set of sampled points. The loess predictions at unsampled points in the Sierra Nevada range were largely influenced by the surrounding passive sampler sites rather than the lower-elevation continuous monitoring sites, which were not as representative of the higher-elevation Sierra Nevada.

The precision in estimating the mean O_3 surface in the western half of the study area was largely unchanged by the inclusion or exclusion of the passive

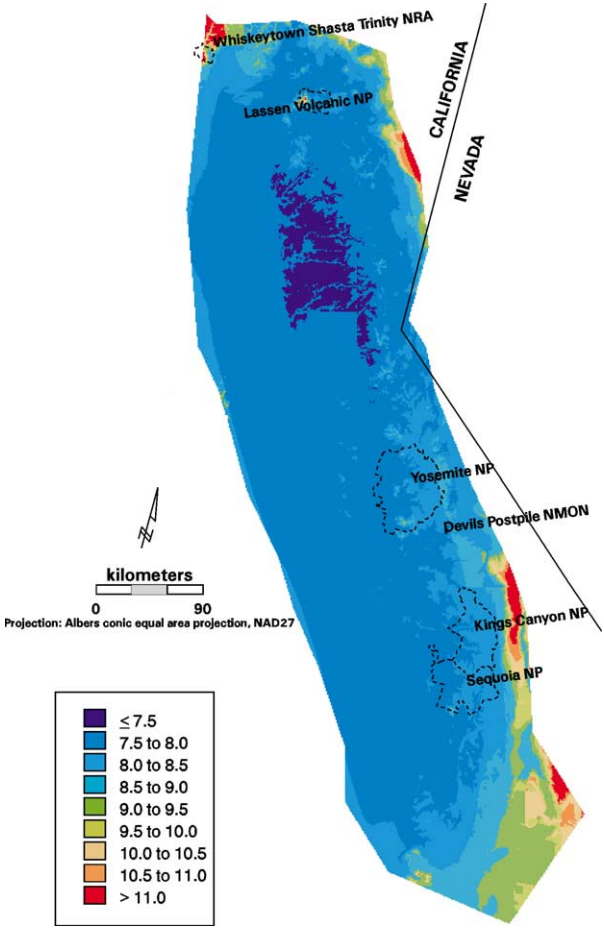

Figure 9. Standard deviation for predicted mean ozone concentration (ppb) for Sierra Nevada study area for the June 9 to September 29, 1999 period based on combined data for continuous monitors and passive samplers.

samplers in the loess fit (Fig. 11). Ratios greater than 1 indicated areas where precision was enhanced with the inclusion of a passive sampler site, and ratios $\leqslant 1$ indicated areas where precision was unchanged. The ratio of the loess SD for estimation of the mean O_3 surface excluding and including the passive sampler data was highest in the northern latitudes of the Sierra Nevada. When the passive samplers were included in the loess regression, precision was typically enhanced by at least a factor of 1.25 in the higher elevations (> 2000 m) in the Sierra Nevada range. These findings indicated that the passive samplers

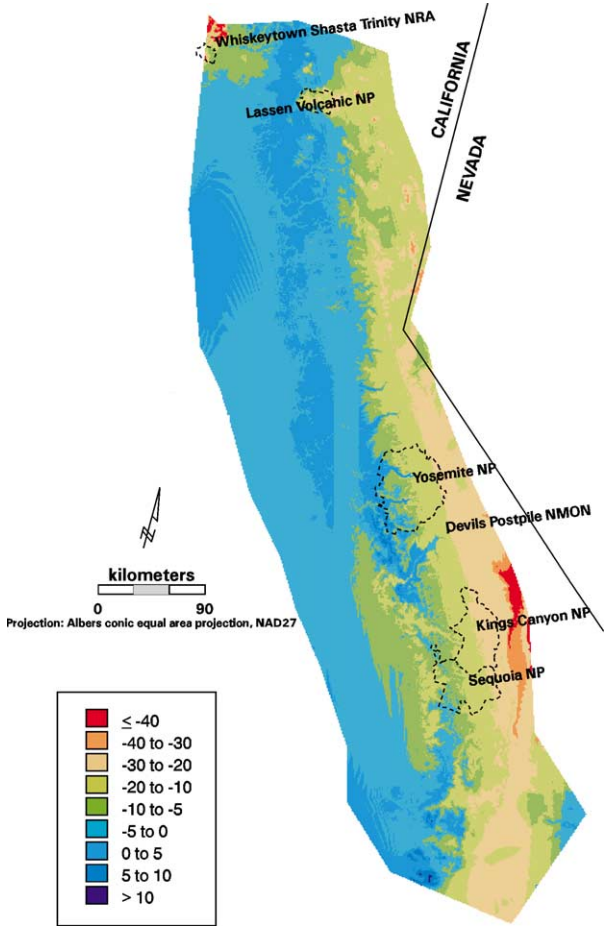

Figure 10. Difference in predicted mean ozone concentration (ppb) for Sierra Nevada study area for period June 9 to September 29, 1999, between continuous monitors and passive samplers.

in the higher elevations of the Sierra Nevada were key in supplementing the continuous monitor network based on increased accuracy and precision.

3.5. Cross-validation of loess ozone predictions

Although the leave-one-out cross-validation results indicated that loess mean O_3 predictions based on only the continuous monitor data were accurate and precise, these findings were not validated at the higher-elevation passive sampler sites (Table 3). There was a tendency to underpredict the mean O_3 concen-

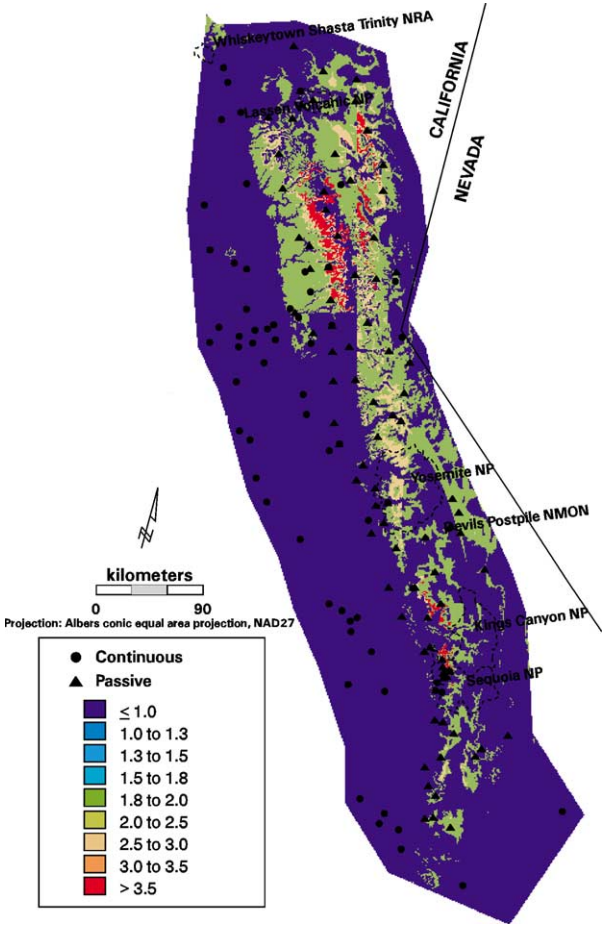

Figure 11. Ratio of loess standard deviation for estimation of mean ozone concentration surface based on continuous ozone monitors alone to that for combined data with passive samplers.

tration by 6.9 ppb, on average, at the higher elevations in the Sierra Nevada. Also, the loess predictions were much less precise at the passive sampler sites (cross-validation standard error = 10.4 ppb) because spatial coverage of the continuous monitoring network was limited in the Sierra Nevada. Only 71% of the observed mean O_3 concentrations at the passive sampler sites fell within the 95% prediction interval. The loess predictions based on the continuous O_3 monitoring network were inadequate because the sampled points typically had strong diurnal patterns commonly found in low-elevation urban areas rather than the less distinct diurnal patterns found in the higher elevations in the

Table 3. Summary of the leave-one-out cross-validation results for the loess prediction of mean ozone concentration for the continuous monitors from the US EPA AIRS and the USDA FS PSWRS SCOIAS and FOREST databases, alone and in conjunction with the passive sampler stations from the USDA FS PSWRS. The passive sampler data were also used to validate the loess predictions based on data from the continuous monitors

Data	Minimum observed, predicted (ppb)	Maximum observed, predicted (ppb)	Mean observed, predicted (ppb)	Mean error (ppb)	Mean |error| (ppb)	Cross-validation std. error (ppb)	Mean pred. SD (ppb)	% of errors within 95% predicted interval	Correlation observed vs predicted
Continuous monitor[1]	23.2, 25.6	66.8, 63.6	43.8, 43.6	−0.1	4.3	5.4	5.4	96.7	0.88
Passive sampler[2]	33.8, 23.6	81.8, 79.7	57.6, 50.7	6.9	10.0	11.4	8.4	71.4	0.48
Continuous monitor[3]	23.2, 26.9	66.8, 80.9	43.8, 45.5	−1.8	4.8	6.1	7.9	98.4	0.86
Passive sampler[3]	33.8, 41.2	81.8, 72.7	57.6, 56.8	0.8	7.4	8.8	7.9	95.1	0.57
Overall[3]	23.2, 26.9	81.8, 80.9	51.6, 51.9	−0.3	6.3	7.8	7.9	96.5	0.80

[1]Loess fit using continuous monitor data only. Leave-one-out cross-validation predictions not possible for two monitoring sites.
[2]Loess fit using continuous monitor data only was used to predict mean ozone concentrations at the passive sampler sites.
[3]Loess fit using combined data. Leave-one-out cross-validation predictions not possible for one continuous monitoring site.

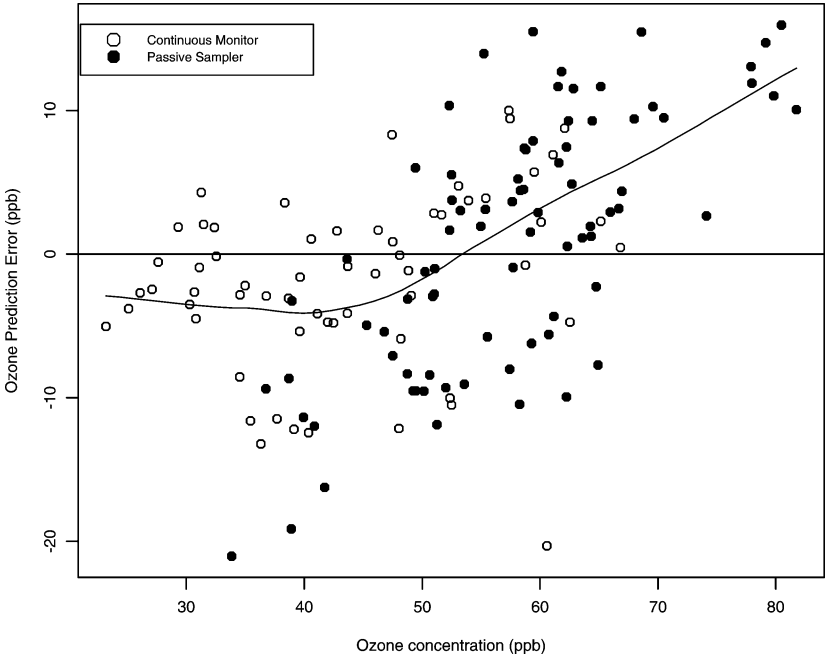

Figure 12. Observed mean ozone concentration versus cross-validation prediction error at 62 continuous monitors and 81 passive sampler sites.

Sierra Nevada range. Mean O_3 concentrations increased with elevation because nighttime and morning concentrations were higher at higher elevations while daytime concentrations were similar at nearby sites.

When the continuous monitor and passive sampler data were combined, the leave-one-out cross-validation results indicated that loess O_3 predictions were accurate and fairly precise for the study area (Table 3). For example, the overall mean error was -0.3 ppb, but there was a tendency to understate the higher O_3 concentrations greater than 67 ppb and overstate the lower O_3 concentrations less than 42 ppb (Fig. 12). Predictions were less accurate and less precise at the passive sampler sites due to a combination of more complex terrain, greater spatial variability, measurement and analytical error, and the inherent variability in the O_3-nitrate formation rate relationship. Nonetheless, the leave-one-out loess predictions based on the combined data at the passive sampler sites were more accurate and precise than predictions based on the continuous monitors. The prediction errors were generally less than 10 ppb in absolute value and 97% of the errors fell within the 95% prediction interval. The correlation between observed and predicted mean O_3 values was 0.80 overall and 0.57 for

the passive samplers. Similar results were obtained by using the 2-week mean O_3 concentrations (not shown).

Meaningful relationships were not found between the prediction errors, geographic location, elevation and temperature, indicating that the loess model based on combined data was appropriate. Large absolute prediction errors for passive sampler sites were likely due to measurement or analytical error rather than to modeling error. The three highest overpredictions coincided with three passive samplers that had very low O_3 concentrations (and NO_3^- formation rates), and the highest underpredictions coincided with passive samplers that had high O_3 concentrations (Fig. 12). In addition, the very low NO_3^- formation rates at four passive sampler sites resulted in underpredicting the mean O_3 concentrations by at least 10 ppb for its nearest neighbors. Prediction errors greater than 10 ppb in absolute value for nine passive sampler sites in the Sequoia National Park and Sequoia National Forest were due to the complex terrain where elevation changed rapidly over short distances. This finding indicates that more intense sampling is needed in the lower latitudes of the Sierra Nevada where elevation gradients are steepest and large biases in O_3 predictions are most likely to occur. Large prediction errors for continuous monitor sites were likely due to edge effects and poor spatial coverage along the periphery of the study area. Prediction errors less than -10 ppb were observed at two isolated continuous monitoring sites located in the northwest corner and southern edge of the study area.

4. Conclusion

The passive O_3 sampler data significantly improved the accuracy and resolution of the loess prediction surface for seasonal mean O_3 concentrations in the Sierra Nevada. Mean O_3 concentrations were less uniform in the higher elevations of the Sierra Nevada than in the low-lying basin of the Central Valley. With the increased spatial resolution of the combined data for continuous monitors and passive samplers, the effects of topographical features that are 50 to 100 km wide on O_3 formation and transport were detected in the loess prediction surface. Prevailing westerly to northwesterly winds transported pollutant plumes from major urban sources in the southern latitudes of the SJV toward the Sierra Nevada foothills, where seasonal mean O_3 concentrations were higher than in the low-elevation Central Valley region sheltered by the coastal range. Mean O_3 concentrations decreased as prevailing winds transported pollutant plumes further away from the major urban sources in the southern latitudes.

Mean O_3 concentrations changed rapidly over short distances as elevation and local topographic settings changed in the Sierra Nevada study area. Higher

mean O_3 concentrations were predicted at higher elevations because of persistently high morning and nighttime concentrations at higher elevations while daytime concentrations were similar at neighboring sites. Similar findings were reported in the Cascade mountains in Mount Rainier National Park (Brace and Peterson, 1998). The large spatial variability of mean O_3 concentrations dominated the prediction standard deviation calculation, resulting in uniformly high prediction standard deviations across the study area. Mean O_3 concentrations tend to be more variable, and therefore more difficult to interpolate, than O_3 exposure indices that focus on the daytime concentrations (e.g., 12-h SUM06 for the 8 AM to 8 PM period).

When the passive sampler data were combined with the continuous monitoring data, the accuracy and precision of the mean O_3 prediction surface improved to varying degrees, depending upon the spacing of the sampled points, complexity of terrain and the spatial distribution of the regionalized variables of interest. The greatest improvement in accuracy and precision occurred at isolated higher elevation passive sampler sites along the eastern periphery and in the northeastern section of the Sierra Nevada where spatial coverage of continuous monitors was lacking. For example, the passive sampler site at Rovana (ID = 405, elevation = 1801 m, mean O_3 concentration = 59 ppb) was significantly underpredicted by 35 ppb based on only the network of continuous monitors. More intense sampling is required in environmentally and topographically complex terrain (e.g., Lassen Volcanic and Yosemite National Parks) where air transport patterns are complex and the variability of O_3 concentrations is high. The leave-one-out cross-validation results indicated that there were a number of redundant passive sampler sites that could be excluded with little or no loss in accuracy or precision of the estimated mean O_3 surface. The cross-validation results further indicated that more intense sampling was required in the southern latitudes of the Sierra Nevada range to reduce the potential bias in areas where elevation gradients were severe. Future research will consider a more formal statistical analysis to design a parsimonious passive sampler network in the Sierra Nevada for purposes of spatial interpolation.

Passive samplers provide a cost-effective solution to the problem with the bias in the location of continuous O_3 monitors towards lower elevations and major urban areas. High-elevation and remote, forested regions are represented poorly by the spatial distribution of continuous monitoring and meteorological networks. The accuracy and precision of the O_3 prediction surface in complex terrain are suspect when the elevation for the sampled points has a much different distribution than that for the study area. The leave-one-out cross-validation results provide, at best, a rough indicator of the accuracy and precision of the interpolated surface within a neighborhood of the sampled points. Passive sampler data provide a much better method for validation of the O_3 predictions based on continuous monitoring data. More importantly, passive O_3 samplers

in conjunction with the active O_3 monitors can be used to predict mean concentrations at a reasonable level of accuracy in mountainous regions.

Acknowledgements

The information in this document has been funded wholly by the US Environmental Protection Agency. It has been subjected to the Agency's peer review and administrative review, and it has been approved for publication as an EPA document. Mention of trade names or commercial products does not constitute endorsement or recommendation for use. The author acknowledges the California Air Resources Board, and the USDA Forest Service's Sierra Nevada EIS for providing partial support in gathering passive sampler data used in this study.

The author acknowledges contribution of passive sampler, active monitor, and meteorological data from Dr. Andrzej Bytnerowicz and Dr. Michael Arbaugh, USDA Forest Service, Pacific Southwest Research Station. The author thanks Jeffrey Kern for providing GIS support and the digital elevation model data from the US Geological Survey.

References

Böhm, M., McCune, B., Vandetta, T., 1991. Diurnal curves of tropospheric ozone in the western United States. Atmos. Environ. 25A, 1577–1590.

Böhm, M., McCune, B., Vandetta, T., 1995. Ozone regimes in or near forests of the western United States: I. Regional patterns. J. Air Waste Manag. Assoc. 45, 235–246.

Brace, S., Peterson, D.L., 1998. Spatial patterns of tropospheric ozone in the Mount Rainier region of the Cascade Mountains, USA. Atmos. Environ. 32, 3629–3637.

Bytnerowicz, A., Fenn, M.E., Miller, P.R., Arbaugh, M.J., 1999. Wet and dry pollutant deposition fo the mixed conifer forest. In: Miller, P.R., McBride, J.R. (Eds.), Oxidant Air Pollution Impacts in the Montane Forests of Southern California: a Case Study of the San Bernardino Mountains. In: Ecological Studies, Vol. 134. Springer-Verlag, New York, pp. 235–269.

Chameides, W.L., Saylor, R.D., Cowling, E.B., 1997. Ozone pollution in the rural US and the new NAAQS. Science 276, 916.

Chock, D.P., Kumar, S., Herrmann, R.W., 1982. An analysis of trends in oxidant air quality in the South Coast Air Basin of California. Atmos. Environ. 16, 2615–2624.

Cleveland, W.S., 1979. Robust locally-weighted regression and smoothing scatterplots. J. Am. Statist. Assoc. 83, 596–610.

Cleveland, W.S., Grosse, E., Shyu, W.M., 1992. Local regression models. In: Statistical Models, Pacific Grove, California. In: Chambers, J.M., Hastie, T.J. (Eds.), Computer Science Series. S. Wadsworth & Brooks/Cole, pp. 309–376.

Cooper, S.M., Peterson, D.L., 2000. Spatial distribution of tropospheric ozone in western Washington, USA. Environ. Pollut. 107, 339–347.

Cressie, N., 1985. Fitting variogram models by weighted least squares. Math. Geol. 17, 563–586.

Demerjian, K.L., 2000. A review of national monitoring networks in North America. Atmos. Environ. 34, 1861–1884.

Dodson, R., Marks, D., 1997. Daily air temperature interpolated at high spatial resolution over a large mountainous region. Climate Res. 8, 1–20.

Earthinfo, 1992. Earthinfo's NCDC summary of the day user's manual. Earthinfo, Inc., Boulder, Colorado.

Eder, B.K., Davis, J.M., Bloomfield, P., 1994. An automated classification scheme designed to better elucidate the dependence of ozone on meteorology. J. Appl. Meteorol. 33, 1182–1199.

Edinger, J.G., 1973. Vertical distribution of photochemical smog in the Los Angeles basin. Environ. Sci. Technol. 7, 247–252.

Fujioka, F.M., Roads, J.O., Chen, S.-C., 1999. Climatology. In: Miller, P.R., McBride, J.R. (Eds.), Oxidant air Pollution Impacts in the Montane Forests of Southern California: a Case Study of the San Bernardino Mountains. In: Ecological Studies, Vol. 134. Springer-Verlag, New York, pp. 28–43.

Guttorp, P., Meiring, W., Sampson, P.D., 1994. A space–time analysis of ground-level ozone data. Environmetrics 5, 241–254.

Kuntasal, G.C., Chang, T.Y., 1987. Trends and relationships of O_3, NO_x, and HC in the South Coast Air Basin of California. J. Air Pollut. Control Assoc. 37, 1158–1163.

Lee, E.H., Hogsett, W.E., 2001. Interpolation of temperature and non-urban ozone exposure at high spatial resolution over the western United States. Climate Res. 18, 163–179.

Logan, J.A., 1989. Ozone in rural areas of the United States. J. Geophys. Res. [Atmos.] 94, 8511–8532.

Loveland, T.R., Merchant, J.W., Ohlen, D.O., Brown, J.F., 1991. Development of a land-cover characteristics database for the conterminous United States. Photogramm. Eng. Remote Sens. 57, 1453–1463.

Ludwig, F.L., Jiang, J.-Y., Chen, J., 1995. Classification of ozone and weather patterns associated with high ozone concentrations in the San Francisco and Monterey Bay areas. Atmos. Environ. 29, 2915–2928.

MathSoft, 1996. S+SPATIALSTATS User's Manual, Version 1.0. MathSoft, Seattle, WA.

MathSoft, 2000. S-PLUS 6 for UNIX Guide to Statistics. Data Analysis Products Division, MathSoft, Seattle, WA.

Miller, P.R., 1996. Extent of ozone injury to trees in the western United States. In: Miller, P.R., Stolte, K.W., Duriscoe, D.M., Pronos, J., tech. coords. Evaluating Ozone Air Pollution Effects on Pines in the Western United States. USDA Forest Service, Pacific Southwest Research Station, Gen. Tech. Rep. PSW-GTR-155, 1-9. Available at the Web site: http://www.psw.fs.fed.us/Tech_Pub/Documents/gtr-155/01-miller.html.

Miller, P.R., Taylor, O.C., Poe, M.P., 1986. Spatial variation of summer ozone concentrations in the San Bernardino Mountains. In: Proceedings 79th Annual Meeting of the Air Pollution Control Association. Air Pollution Control Association, Pittsburgh, PA.

National Research Council, 1992. Rethinking the ozone problem in urban and regional air pollution. National Academy Press, Washington, D.C. Available at the Web site: http://www.nap.edu/index.html.

Oke, T.R., 1990. Boundary Layer Climates. Routledge, London.

Peterson, D.L., Bowers, D., Brace, S., 1999. Tropospheric ozone in the Nisqually River drainage, Mount Rainier National Park. Northwest Sci. 73, 241–254.

Ray, J.D., 1993. Field Use of the Passive Ozone Aamplers, Standard Operating Procedure Document. National Park Service, Air Resources Division, Denver, CO.

Ray, J.D., 1996. Ambient Ozone Measurements in the National Parks Using Passive Samplers, 1995–1996. National Park Service, Air Resources Division, Denver, CO. Available at the Web site: http://www.aqd.nps.gov/ard/gas/ps56rprt.pdf.

Ray, J.D., 2001. Spatial distribution of tropospheric ozone measurements in national parks of California: interpretation of passive-sampler data. Proceedings of the International Symposium on Passive Sampling of Gaseous Air Pollutants in Ecological Effects Research. The Scientific World 1, 483–497.

Ray, J.D., Flores, M.I., 1994. Passive Ozone Sampler Study II: 1993 Results. National Park Service, Air Resources Division, Denver, CO.

Saylor, R.D., Chameides, W.L., Cowling, E.B., 1998. Implications of the new ozone National Ambient Air Quality Standards for compliance in rural areas. J. Geophys. Res. 103, 31137–31141.

Van Ooy, D.J., Carroll, J.J., 1995. The spatial variation of ozone climatology on the western slope of the Sierra Nevada. Atmos. Environ. 29, 1319–1330.

Wolff, G.T., Lioy, P.J., 1978. An empirical model for forecasting maximum daily ozone levels in the northeastern US. J. Air Pollut. Control Assoc. 28, 1034–1038.

Wolff, G.T., Lioy, P.J., Taylor, R.S., 1987. The diurnal variations of ozone at different altitudes on a rural mountain in the Eastern United States. J. Air Pollut. Control Assoc. 37, 45–48.

Zhou, J., Smith, S., 1997. Measurement of ozone concentrations in ambient air using a badge-type passive monitor. J. Air Waste Manage. Assoc. 47, 697–703.